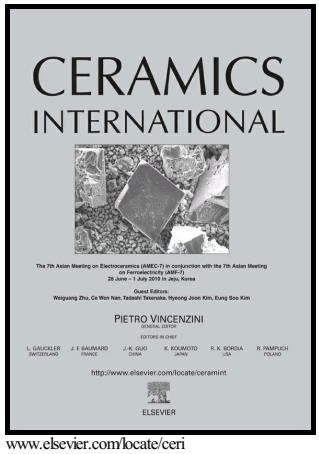

www.elsevier.com/locate/ceri

Microwave-Assisted Synthesis of Ce-Doped ZnO/CNT Composite with Enhanced Photo-catalytic Activity

Md. Elias, Md. Khairul Amin, Shakhawat H. Firoz, Md. Asjad Hossain, Sonia Akter, Md. Awlad Hossain, Md. Nizam Uddin, Iqbal Ahmed Siddiquey

PII: S0272-8842(16)31640-6
DOI: http://dx.doi.org/10.1016/j.ceramint.2016.09.114
Reference: CERI13774

To appear in: *Ceramics International*

Received date: 20 July 2016
Revised date: 6 September 2016
Accepted date: 16 September 2016

Cite this article as: Md. Elias, Md. Khairul Amin, Shakhawat H. Firoz, Md Asjad Hossain, Sonia Akter, Md. Awlad Hossain, Md. Nizam Uddin and Iqbal Ahmed Siddiquey, Microwave-Assisted Synthesis of Ce-Doped ZnO/CNT Composite with Enhanced Photo-catalytic Activity, *Ceramics International* http://dx.doi.org/10.1016/j.ceramint.2016.09.114

Microwave-Assisted Synthesis of Ce-Doped ZnO/CNT Composite with Enhanced Photo-catalytic Activity

Md. Elias[a,b], Md. Khairul Amin[b,c], Shakhawat H. Firoz[d], Md. Asjad Hossain[b], Sonia Akter[b], Md. Awlad Hossain[a], Md. Nizam Uddin[b], Iqbal Ahmed Siddiquey[b]*

[a]Department of Chemistry, Jagannath University, Dhaka 1100, Bangladesh
[b]Department of Chemistry, Shahjalal University of Science and Technology, Sylhet 3114, Bangladesh
[c]Chemistry Discipline, Khulna University, Khulna 9208, Bangladesh
[d]Department of Chemistry, Bangladesh University of Engineering and Technology, Dhaka 1000, Bangladesh
*Corresponding author. *Postal address:* Department of Chemistry, Shahjalal University of Science and Technology, Sylhet-3114, Bangladesh. Tel.: 880-821-716123 (Ext 436), *E-mail address*: iqbal_siddiquey@yahoo.com (Iqbal Ahmed Siddiquey)

Abstract

This manuscript reports a successful additive free and fast energy-efficient microwave-assisted synthesis of nanocrystalline Ce-doped ZnO/CNT composite without calcinations. The structure and morphology of nanocrystalline Ce-doped ZnO/CNT was investigated by X-ray Diffraction (XRD), Field Emission Scanning Electron Microscope (FESEM), Fourier Transform Infrared Spectroscopy (FT-IR), UV-visible and Photoluminescence (PL) spectroscopy. The XRD results indicate that all of the samples are free of any impurity phase and crystallize only in the hexagonal structure. The synthesized Ce-doped ZnO/CNT composite achieved 96.4% photo-catalytic efficiency for methylene blue (MB) dye degradation under UV irradiation whereas the efficiency was only 34.6 % for pure ZnO nanoparticles. Ce doping and insertion of CNTs into ZnO matrix enhanced the photo-catalytic activity of the composite by reducing the charge recombination. The experimental photodegradation data were well fitted to first-order, parabolic diffusion and modified Freundlich models. The results suggest that Ce-doped ZnO/CNT composite prepared by microwave irradiation method has a potential application in photo-catalysis which leads to the removal of harmful organic pollutant from the environment.

Keywords: Composites; Microwave processing; Functional applications; Optical properties

1. Introduction

Heterogeneous photo-catalysis is considered as an effective method for the complete degradation of organic and inorganic pollutants by producing electron hole pairs after adsorption of a photon at ambient temperature and pressure [1–3]. ZnO is a wide band gap semiconductor (3.37 eV) photocatalyst with large exciton binding energy of 60 meV [4]. ZnO-based photocatalysts have been studied extensively because of their excellent properties, such as high chemical stability, good optical and electrical response, nontoxicity, and abundance in nature [5,6]. However, a major drawback of achieving high photo-catalytic efficiency is the quick recombination of photo-generated charge carriers that greatly reduces the quantum efficiency of photo-catalysis. To overcome this limitation, a variety of methods, such as the metal doping, noble metal deposition, semiconductor coupling, dye sensitizing, and non-metal modification, have been developed [7–10]. Among these methods, doping with metal is the most effective to enhance photo-catalytic properties of ZnO in order to extend its practical applications.

A numerous investigations have been reported on the utilization of several metals such as Fe[6], Pd[5], W[11], Se[12], Al[10], Cu[13], Ag[14] and Sb[7] to tune the desirable properties of ZnO. In addition to these metal doping, the rare earth metal, like Ce displays a high surface basicity, fast oxygen ion mobility and substancial catalytic properties which make ZnO as a suitable candidate for enhancing photo-catalytic properties [15]. Ismail et al. [16] reported the synthesis of Ce-doped ZnO under mild hydrothermal conditions utilizing polyamines triethylenetetraamine and observed the higher degradation of MB under UV irradiation than pure ZnO. Both Lijuan et al. [17] and Jiantai et al. [18] synthesized highly uniform $NiCo_2O_4$@CeO_2 and TiO_2@h-CeO_2 core@shell nano composites and studied their enhanced photo-catalytic efficiencies. Chaorong et al. [19] fabricated CeO_2-ZnO nanofibers by electrospinning method and evaluated the effective photo-catalytic activity by degradation of Rhodamine B. Yousefi et al. [20] and Shi et al. [21] synthesized Ce-doped ZnO by sol-gel method and studied photo-electrochemical activity as well as monitored luminescence properties. Shanthi et al. [22] reported the solvothermal synthesis of Ce co-doped Ag-ZnO photocatalyst and demonstrated that that the prepared material showed more efficient photo-catalytic activity than Ag-ZnO, Ce-ZnO, commercial and synthesized ZnO, TiO_2-P25 and TiO_2 (Merck) for the degradation of Naphthol blue black dye under solar light irradiation.

The aim of this present work is to develop an inexpensive, facile and fast microwave-assisted synthesis technique to fabricate a Ce-doped ZnO/CNT composite. As a new carbonaceous material, carbon nanotube (CNT) with unique properties such as high aspect ratio, high surface

area to volume ratio, ability to be substituted chemically, high electro-catalytic effect, strong adsorptive ability, excellent biocompatibility, good optical and electronic response, have been regarded as promising candidate for various applications [23,24]. CNTs have a large electron-storage capacity (one electron for every 32 carbon atoms) and therefore may accept photon-excited electrons in mixtures or nanocomposites with ZnO thereby retarding the recombination and synergistically enhance the photo-catalytic activity [25,26].

Up to date, very few works have been reported on photo-catalytic degradation by metal-doped ZnO/CNT composites. Moreover, most of the reported methods of Ce-doped ZnO as well as metal-doped ZnO/CNT required the use of high temperature, long reaction time and high pressure. These reported methods of composite fabrication involve the use of environmentally malignant chemicals and organic solvents, which are toxic and not easily degradable in the environment [15,27]. Therefore, there has been a strong demand to design a facile, rapid, convenient, low-cost, green and additive free method.

The microwave (MW) irradiated method has been shown to offer a number of benefits over conventional solution method such as rapid and homogeneous heating, mild reaction conditions and drastically short reaction time. Recently, MW energy has been effectively used in the field of materials science for synthesizing various composite ceramic powders at far lower temperatures and shorter time periods compared to conventional methods [28,29].

Herein we reported a facile, additive free microwave-assisted protocol for the synthesis of Ce-doped ZnO/CNT composite using water, zinc acetate and CNT suspension. To the best of our knowledge, this is the first report on the additive free microwave-assisted synthesis of Ce-doped ZnO/CNT composite. The photo-catalytic performance of as-synthesized Ce-doped ZnO/CNT composite was investigated by degradation of methylene blue (MB) under UV irradiation as compared with pure ZnO and Ce-doped ZnO.

2. Experimental Section

2.1. Materials

All chemicals and reagents were analytical grade and used without further purification. Zinc acetate dihydrate ($Zn(CH_3COO)_2 \cdot 2H_2O$, Merck, Germany), sodium hydroxide, cerium sulfate and methylene blue (MB) were purchased from Sigma-Aldrich. Multi-walled carbon nanotubes

(MWCNTs) were also purchased from Sigma-Aldrich with detailed specifications as follows: length (5-9 μm), diameter (110-170 nm) and assay > 90% (carbon basis).

2.2. Sample Preparation

Functionalization of MWCNTs was carried by immersing 1.0 g of MWCNTs into a 40 ml mixed solution of concentrated sulphuric acid and nitric acid with a volume ratio of 1:1. The mixture was then heated to 70-80°C for 5 hours under refluxing to get dark-brown suspension which was cooled naturally to room temperature. The MWCNTs were then filtered and washed with distilled water until the pH of the filtered solution was about 6-7. The product was then dried at 80°C in an oven and kept in desiccators.

Pure ZnO was prepared by MW irradiating of the solution containing 0.05 M zinc acetate, water and sodium hydroxide. Ce-doped ZnO composite was prepared by the same method using microwave with the addition of 5% wt Ce into 0.05 M zinc acetate solution. To synthesize Ce-doped ZnO/CNT, initially 5 wt% CNT and 5 wt% Ce were added into 100 ml 0.05 M zinc **acetate solution and the solution was sonicated (Powersonic 405, Hwashin technology Co., Korea) for 1 h to get a uniform dispersion. An aqueous solution of NaOH (5 M) was added drop-wise into the solution until the pH value reached 11. Then the solution was placed in a domestic microwave oven (Samsung Engineering Co., Korea) with a microwave stirrer (Bel Art Scienceware Co., USA) which was operated at 450W and a frequency of 2.45 GHz for 5** minutes. The as-synthesized Ce-doped ZnO/CNT sample was isolated by centrifugation followed by washing several times with distilled water and ethanol. Finally, the sample was dried in an oven at 80 ºC for 12 h.

2.3. Samples Characterization

The crystalline structure of prepared samples was analyzed by XRD using Cu-K_α radiation (λ=1.5406 Å). The morphology of the prepared samples was investigated with a Field Emission Scanning Electron Microscope (FESEM, JEOL JSM-7600F). Point and shoot analyses were applied to determine the presence of elements in the samples by Energy-dispersive X-ray spectroscopy (EDS).

The absorption spectra of the prepared samples were investigated by UV-visible spectroscopy (UV-1800, Shimadzu, Japan). FT-IR spectra were recorded in transmission mode on KBr pellets using a Prestige-21spectrometer (Shimadzu Corp., Japan). The Photoluminescence (PL)

properties of synthesized samples were measured by a spectrofluorophotometer (RF-5301, Shimadzu Corp., Japan) in ethanol.

2.4. Photo-catalytic studies

The photocatalytic activities of the samples were evaluated by measuring the photodegradation of methylene blue(MB). Experimental process was as follows: the powder samples (50 mg) were added to a 100 ml of methylene blue (MB) aqueous solution (5 mg/L). In all experiments, the aqueous solution was stirred continuously in the dark for 60 min to ensure adsorption/desorption equilibrium and then irradiated. Under ambient conditions and constant stirring it was subjected to UV irradiation (60 W low pressure mercury lamp; 362 nm). The distance between the dye solution and the light source was kept within 25 cm. Samples were taken at a regular interval by a syringe and after centrifugation, the absorbance of the MB solution at 664 nm was measured using a UV–vis spectrophotometer to determine the residual concentration. The photo-degradation efficiency (%) of MB was calculated using the following equation:

$$\text{Efficiency (\%)} = (C_0 - C_t)/C_0 \times 100 \approx (A_o - A_t)/A_o \times 100 \quad (1)$$

where A_0 is the absorbance of MB before the treatment and A_t is that of after treatment at time t.

Four kinetic models were employed to study the photodegradation process [30].

The zero-order model describes the dissolution process and can be generally expressed as:

$$C_t - C_0 = -kt \quad (2)$$

The first-order model expresses the photo-catalytic dissolution degradation by systems and can be generally written as:

$$\log (C_t/C_o) = -kt \quad (3)$$

The parabolic diffusion model elucidates the diffusion controlled photo-catalytic degradation and the equation is as follows:

$$(1- C_t/C_o)/t = kt^{-0.5} + a \quad (4)$$

The modified Freundlich model explains experimental data on ion exchange process with the following equation:

$$(C_t - C_0)/C_0 = kt^b$$

$$\log (1- C_t/C_o) = \log k + b \log t \quad (5)$$

In these equations, C_o and C_t are the concentration of MB at irradiation time '0' and 't', respectively, k the corresponding rate constant, and a and b constants [30].

3. Results and Discussion

3.1. FT-IR analysis

Functionalization of CNTs plays an important role in facilitating the binding of ZnO NPs on the surface of CNTs since it introduces chemical functional groups to the surface of nanotubes. The polar groups like hydroxyl or carboxyl on the functionalized CNTs surface are then able to interact with the oxygen of the ZnO NPs. The interaction could be through hydrogen bonding, or the oxygen atoms of hydroxyl or carboxyl groups interact with Zn atoms through the pair of electrons on the oxygen atoms. The formation of chemical bond is also possible.

FTIR is used to analyze the chemical bonding and type of functional groups grafted onto the nanotubes. Fig. 1 shows the FTIR spectra of pure and acid treated functionalized-MWCNTs (FMWCNTs) respectively. The FTIR spectrum of functionalized CNTs exhibits absorption peak at 1715 cm^{-1} corresponding to the stretching vibration of C=O from the carboxylic groups (–COOH). The carbonyl characteristic peak is also observed at about 1636 cm^{-1} and can be assigned to the carbonyl group from quinine or ring structure. The broad peaks at 1180 cm^{-1} could be assigned to C–O stretch from phenol or lactone groups and also to C–C bonds. The band at 2910 cm^{-1} and 2850 cm^{-1} corresponds to C-H stretching. The peak at around 3400 cm^{-1} corresponds to O-H stretching. This peak can be assigned to the hydroxylic group of moisture, alcohol, or carboxylic groups. The aromatic C=C stretch is observed at around 1580 cm^{-1} in spectra of both pure CNTs and FMWCNTs [32,33]**.**

The peaks at 899 cm^{-1} and 442 cm^{-1} indicate the presence of O-Zn-O and Zn-O stretching respectively (Fig. 2 (a)). The origin of two bands at 1119 cm^{-1} and 620 cm^{-1} due to O-Ce-O and Zn-O stretching respectively indicate the successful doping of ZnO by Ce (Fig. 2(b) and (c). It is remarkable that the band position of doped samples are slightly shifted to the higher wavenumber, this may be due to the change in particles size or degree of aggregation during doping [35,36]. No other absorption band except mentioned here was detected in FTIR spectra

which substantiates that the synthesized samples are almost pure without any significant impurity.

3.2. XRD analysis

Fig. 3 shows the XRD patterns of pure ZnO, Ce-doped ZnO and Ce-doped ZnO/CNT photocatalysts. All prepared samples showed a hexagonal wurtzite crystal structure and high crystallinity of ZnO photocatalyst (JCPDS No. 01-075-0576). The prominent peaks labeled at 31.93°, 34.57°, 36.43°, 47.57°, 56.75°, 62.95°, 66.51° 68.11° and 69.35° correspond to the (100), (002), (101), (102), (110), (103), (200), (112) and (201) planes, respectively, confirming the formation of hexagonal zinc oxide phase [5,11]. As can be seen, the XRD patterns for Ce-doped ZnO and Ce-doped ZnO/CNT nanostructures are almost similar to pure ZnO and no diffraction peaks associated to Ce and other related impurities such as CeO_2, Ce_2O_3 or other crystalline forms were identified. Then, it can be concluded that Ce^{4+} ions would uniformly substitute into the Zn^{2+} sites or interstitial sites in ZnO lattice. However, the sharp diffraction peaks reveal that the as-prepared pure ZnO, Ce-doped ZnO and Ce-doped ZnO/CNT nanostructures have high crystallinity [15]. No characteristic diffraction peaks of CNT are detected due to the low amount of CNT in the composite [9]. In addition to the identification of the crystalline phase, the XRD data were used to estimate average size of the crystallites, *D*, calculated from the peak half-width β, using the by Scherrer's equation [5]**,**

$$D = \frac{k\lambda}{\beta \cos\theta} \quad (6)$$

where *k* is a shape factor of the particle, λ and θ are the wavelength and the incident angle of the X-rays, respectively. The average crystal size is calculated as 42 nm, 35 nm and 25 nm for pure ZnO, Ce-doped ZnO and Ce-doped ZnO/CNT respectively.

3.3. FESEM and EDS analysis

Fig. 4 shows the FESEM images of pure ZnO, Ce-doped ZnO and Ce-doped ZnO/CNT. It is clear from Fig. 4 (a) that the pure ZnO is composed of spherical particles with significant aggregation, while the morphology of Ce-doped ZnO is apparently different (Fig. 4 (b)). After incorporation of Ce-ions into the ZnO matrix, the morphology turns into nano rods with some aggregation. However, the morphology of Ce-doped ZnO/CNT (Fig. 4 (c)) reveals that the

particles are now mostly isolated nano rods. In the liquid-phase chemical synthesis method, in addition to the internal structures, morphology, and microstructure of ZnO crystal are affected by peripheral conditions like precursor, pH value and reaction temperature [37]. The morphology of ZnO changes from spherical to rod shaped with the Ce ion doping because of the fact that crystal lattice spacing of (100) and (101) crystal face shrinks and (002) expands when Ce substituting for Zn sites. In addition, incorporation of CNT also promotes the growth of rods.

To determine the elemental composition of Ce-doped ZnO/CNT composite, the EDS analysis was carried out results obtained are depicted in Fig. 4(d). The spectrum reveals the presence of Zn, O, C, and Ce the absence of other elements, confirming that the synthesized composite is Ce-doped ZnO/CNT. The percentages of the atomic compositions of Zn, O, C and Ce are presented in the Table 1.

3.4. UV-Vis absorption spectra

Fig.5 shows UV-Vis absorption spectra of pure ZnO, Ce-doped ZnO, and Ce-doped ZnO/CNT dispersed in absolute ethanol. The spectra were recorded from 800 nm to 300 nm, giving an absorption peak at 368 nm, 371 nm and 380 nm for pure ZnO, Ce-doped ZnO and Ce-doped ZnO/CNT nano composites, respectively. A small red-shift in the case of Ce-doped ZnO and Ce-doped ZnO/CNT compared to that of pure ZnO reveals the existence of a chemical interaction between dopant and CNT with ZnO NPs. The similar observation was reported in the case of ZnO-reduced graphene oxide-CNT and TiO_2-CNT composites [9,38,39]. These absorption peaks indicate that the particle size of prepared samples are in nano region [40,41]. The band gap of the synthesized samples was found to be 3.37, 3.33 and 3.26 eV for pure ZnO, Ce-doped ZnO and Ce-doped ZnO/CNT, respectively. The general relationship between the band gap energy, E_g (eV) of ZnO and its wavelength, λ (nm) is given by the equation, $E_g = 1240 / \lambda$. It is evident that higher value of wavelength is associated with lowering of the band gap.

3.5. Photoluminescence analysis

Fig. 6 depicts the room-temperature PL spectra of the pure ZnO, Ce-doped ZnO and Ce-doped ZnO/CNT at the excitation wavelength of 325 nm. All PL spectra showed a similar pattern with three emission bands around at 378-382 nm (near band edge emission), 467 nm (blue-green emission) and 547 nm (green emission). The sharp band at 378-382 nm corresponds to the near band edge (NBE) emission, which is attributed to excitonic recombinations [42–44]. The blue-green emission peak at 467 nm in visible region may originate from the direct recombination of electrons in Zn 4p conduction band with holes in O 2p valence band. However, the green emission peak at 547 nm attributed to the presence of many point defects, such as oxygen vacancies [36]. As compared with the spectrum of pure ZnO, the PL peak of Ce-doped ZnO and Ce-doped ZnO/CNT composite displays a red shift, which is consistent with the results of UV-vis absorption spectra. Furthermore, the introduction of CNT decreases the excitonic PL intensity which indicates that the recombination of photo-induced electrons and holes in ZnO can be effectively inhibited in the composite. Photo-catalytic activity is closely related to the lifetime of photo-excited electron-hole pairs [45].

3.6. Evaluation of photo catalytic efficiency

The photo-catalytic activities of the prepared pure ZnO, Ce-doped ZnO and Ce-doped ZnO/CNT catalysts were evaluated by the photo-catalytic degradation of MB dye as a representative organic pollutant in presence of UV irradiation (Fig.7 (a)). Ce-doped ZnO/CNT composite showed 96.4% degradation efficiency at 240 min irradiation while degradation efficiencies of pure ZnO and Ce-doped ZnO were 34.6% and 67.5%, respectively. **The elevated photocatalytic activity may be due to the effective electron transfer between the CNTs and the doped ZnO nanoparticles. A possible synergistic effect between the Ce-doped ZnO nanoparticles and CNTs on the enhancement of photocatalytic activity is schematically presented in Fig. 8. When the ZnO is illuminated by UV photons, electrons (e-) are excited from the valence band (VB) to the conduction band (CB) of the ZnO NPs creating a charge vacancy or holes (h+), in the VB. Cerium plays an important role in the movement of photogenerated electrons and simplifies the separation process of e^-/h^+ pair. In the absence of CNTs, rapid recombination results in a low photocatlytic activity because of only a small fraction of e^-/h^+ participated in the photo-catalytic reactions. In the case of Ce-doped ZnO/CNT composite, the strong interaction between the CNTs and the Ce-doped ZnO results in a**

close contact to form a barrier junction which offers an effective route of reducing electron-hole recombination by improving the injection of electrons into the CNTs [46]**. Therefore, CNTs acts as a favorable reactant-product mass transport system since CNTs are relatively good electron acceptor while the ZnO is an electron donor under irradiation. In addition, stronger adsorption on photocatalyst for the targeted molecules of pollutant is achieved by the incorporation of the nanotubes due to their large specific surface area and high quality active sites** [47,46]**. The adsorbed oxygen molecules on the CNTs react with the electrons forming very reactive superoxide radical ion (O_2•-) which oxidize the target pollutant. On the other side, the hole (h^+) oxidize hydroxyl groups to form hydroxyl radical (•OH) which can degraded the target pollutant.**

The photo-catalytic efficiency of the Ce-doped ZnO/CNT composite and previously reported composite photocatalysts is compared in Table 2.

Four kinetics models viz. zero-order, first-order, parabolic diffusion and modified Freundlich model were applied and calculated at the corresponding linear correlation coefficient (R^2) (Fig.9; Table 3). These kinetic data indicate that the zero-order model is not eligible to explain the entire system (Fig. 9a), whereas first-order, parabolic diffusion and modified Freundlich models fit the experimental photodegradation data quite well. A detailed examination of data point distribution suggests that the whole photo-catalytic degradation process consists of mono linear modeling. The modified Freundlich model describes heterogeneous diffusion from the flat surfaces to the solvent using a composition gradient. This result suggests that (i) the system is controlled by the adsorption-desorption of MB on the ZnO surface and (ii) the photo-catalytic degradation of the dye molecules occur on the ZnO surface. The first order rate constant follows the order as Ce-doped ZnO/CNT (0.00579 min^{-1}) > Ce-doped ZnO (0.00211min^{-1}) > pure ZnO (0.00072 min^{-1}) respectively. Ce-doped ZnO/CNT shows the best photocatalytic activity compared to Ce-doped ZnO and pure ZnO under UV light irradiation.

4. Conclusions

In this work, a new kind of nanocrystalline Ce-doped ZnO/CNT composite was successfully synthesized through a single-step via microwave-assisted method. Different experimental data confirm that the synthesized composite is free of any impurity phase and crystallize in the hexagonal structure with a disperse nano rod as surface morphology. The as prepared Ce-doped ZnO/CNT composite shows highest photo-ctalytic efficiency in MB dye degradation compared with Ce-doped ZnO and and pure ZnO NPs. This was possibly due to the assemblage of

exceptional properties by CNT support and Ce dopant. The appearance of CNT could generate numerous active sites and increase surface area while Ce doping enhanced the separation of photo-generated carriers because of Ce^{3+}/Ce^{4+} ion substitution. Overall, this reported method offers a facile and effective approach of synthesizing Ce-doped ZnO/CNT composite.

Funding

This research was funded by the following projects; (i) Ministry of Science and Technology (MOST), Bangladesh, ref. 39.009.006.01. 00.049.2013–2014/PHY'S-17/331, (ii) The World Academy of Sciences (TWAS) (ref. 13-120RG/CHE/AS_I; UNESCOFR: 3240277720).

Acknowledgements

Authors would like to acknowledge Mr. Ratan Kumar Pal, Assistant Professor, Department of Chemistry, Pabna University of Science and Technology, Pabna for his kind co-operation during the preparation of this manuscript. Shahjalal University of Science & Technology, Sylhet is also acknowledged to give the opportunity to have done this work successfully.

References

[1] M.N. Uddin, M.S. Islam, M.M.R. Mazumder, M.A. Hossain, M. Elias, I.A. Siddiquey, M.A.B.H. Susan, D.K. Saha, M.M. Rahman, A.M. Asiri, S. Hayami, Photocatalytic and antibacterial activity of B/N/Ag co-doped CNT-TiO_2 composite films, J. Incl. Phenom. Macrocycl. Chem. 82 (2015) 229-234.

[2] M.N. Uddin, S.U.A. Shibly, R. Ovali, Saiful Islam, M.M.R. Mazumder, M.S. Islam, M.J. Uddin, O. Gulseren, E. Bengu, An experimental and first-principles study of the effect of B/N doping in TiO_2 thin films for visible light photo-catalysis, J. Photochem. Photobiol. A Chem. 254 (2013) 25-34.

[3] S.-L. Lo Ying-Chu Chen, Effects of operational conditions of microwave-assisted synthesis on morphology and photocatalytic capability of zinc oxide, Chem. Eng. J. 170 (2011) 411-428.

[4] C.L. ChangChun Chen, Ping Liu, Synthesis and characterization of nano sized ZnO powders by direct precipitation method, Chem. Eng. J. 144 (2008) 509-513.

[5] J. Zhong, J. Li, X. He, J. Zeng, Y. Lu, W. Hu, K. Lin, Improved photocatalytic performance of Pd-doped ZnO, Curr. Appl. Phys. 12 (2012) 998-1001.

[6] M.M. Ba-abbad, A. Amir, H. Kadhum, A. Bakar, M.S. Takriff, Visible light photocatalytic activity of Fe^{3+} doped ZnO nanoparticle prepared via sol-gel technique, Chemosphere. 91 (2013) 1604-1611.

[7] A. Omidi, A. Habibi-yangjeh, M. Pirhashemi, Application of ultrasonic irradiation method for preparation of ZnO nanostructures doped with Sb^{+3} ions as a highly efficient photocatalyst, Appl. Surf. Sci. 276 (2013) 468-475.

[8] H. Sun, S. Liu, S. Liu, S. Wang, A comparative study of reduced graphene oxide modified TiO_2, ZnO and Ta_2O_5 in visible light photocatalytic/photochemical oxidation of methylene blue, "Applied Catal. B, Environ. 146 (2014) 162-168.

[9] T. Lv, L. Pan, X. Liu, Z. Sun, Enhanced photocatalytic degradation of methylene blue by ZnO–reduced graphene oxide–carbon nanotube composites synthesized via microwave-assisted reaction, Catal. Techno. 2 (2012) 2297-2301.

[10] M. Ahmad, E. Ahmed, Y. Zhang, N.R. Khalid, J. Xu, M. Ullah, Z. Hong, Preparation of highly ef fi cient Al-doped ZnO photocatalyst by combustion synthesis, Curr. Appl. Phys. 13 (2013) 697-704.

[11] H. Fallah, M.A. Zanjanchi, A.F. Shojaie, Tungsten-doped ZnO nanocomposite : Synthesis , characterization , and highly active photocatalyst toward dye photodegradation, Mater. Chem. Phys. 139 (2013) 856-864.

[12] B.P. Nenavathu, A.V.R.K. Rao, A. Goyal, A. Kapoor, R.K. Dutta, Synthesis, characterization and enhanced photocatalytic degradation efficiency of Se doped ZnO nanoparticles using trypan blue as a model dye, "Applied Catal. A, Gen. 459 (2013) 106-113

[13] P. Jongnavakit, P. Amornpitoksuk, S. Suwanboon, N. Ndiege, Preparation and photocatalytic activity of Cu-doped ZnO thin films prepared by the sol–gel method, Appl. Surf. Sci. 258 (2012) 8192-8198.

[14] R. Georgekutty, M.K. Seery, S.C. Pillai, A Highly Efficient Ag-ZnO Photocatalyst : Synthesis , Properties , and Mechanism, J. Phys. Chem. C. 112 (2008) 13563-13570.

[15] A.H.-Y. M. Rezaei, Simple and large scale refluxing method for preparation of Ce-doped ZnO nanostructures as highly efficient photocatalyst, Appl. Surf. Sci. 265 (2013) 591-596.

[16] M. Faisal, A.A. Ismail, A.A. Ibrahim, H. Bouzid, S.A. Al-Sayari, Highly efficient photocatalyst based on Ce doped ZnO nanorods: Controllable synthesis and enhanced photocatalytic activity, Chem. Eng. J. 229 (2013) 225-233.

[17] Z. Cheng, M. Yu, G. Yang, L. Kang, Fabrication of $NiCo_2O_4$@CeO_2 core@shell nanotubes with enhanced catalytic performances, CrystEngComm. 18 (2016) 6331-6335.

[18] B. Yuan, Y. Long, L. Wu, K. Liang, H. Wen, S. Luo, H. Huo, H. Yang, J. Ma, TiO_2@h-CeO_2 :a composite yolk–shell microsphere with enhanced photodegradation activity, Catal. Sci. Technol. 6 (2016) 6396-6405.

[19] W.D. Chaorong Li, Rui Chen, Xiaoqiang Zhang, Shunxin Shu, Jie Xiong, Yingying Zheng, Electrospinning of CeO_2-ZnO composite nanofibers and their photocatalytic property, Mater. Lett. 65 (2011) 1327-1330.

[20] M. Yousefi, M. Amiri, R. Azimirad, A.Z. Moshfegh, Enhanced photoelectrochemical activity of Ce doped ZnO nanocomposite thin films under visible light, J. Electroanal. Chem. 661 (2011) 106-112.

[21] Q. Shi, C. Wang, S. Li, Q. Wang, B. Zhang, W. Wang, J. Zhang, H. Zhu, Enhancing blue luminescence from Ce-doped ZnO nanophosphor by Li doping, Nanoscale Res. Lett. 9 (2014) 480(9).

[22] B. Subash, B. Krishnakumar, R. Velmurugan, M. Swaminathan, M. Shanthi, Synthesis of Ce co-doped Ag–ZnO photocatalyst with excellent performance for NBB dye degradation under natural sunlight illumination, Catal. Sci. Technol. 2 (2012) 2319-2326.

[23] T.S. Zhao, Micro Fuel Cells: Principles and Applications, 2009.

[24] S.U.N. Fang, L.I.U. Peng, L.I. Li, L. Yong-fu, Non-enzymatic Glucose Biosensor Based on Cu / SWNTs Composite Film Fabricated by One-step Electrodeposition, CHEM. RES. CHINESE Univ. 27 (2011) 1049-1054.

[25] C.S. Chen, T.G. Liu, L.W. Lin, X.D. Xie, X.H. Chen, Q.C. Liu, B. Liang, W.W. Yu, C.Y. Qiu, Multi-walled carbon nanotube-supported metal-doped ZnO nanoparticles and their photocatalytic property, J Nanopart Res. 15 (2013) 1295-5.

[26] A.K. and P. V. Kama, Electron Storage in Single Wall Carbon Semiconductor – SWCNT Suspensions, ACS Nano. 1 (2007) 13–21.

[27] M.A. Bhosale, K.D. Bhatte, B.M. Bhanage, A rapid , one pot microwave assisted synthesis of nanosize cuprous oxide, Powder Technol. 235 (2013) 516-519.

[28] I.A. Siddiquey, T. Furusawa, M. Sato, K. Honda, N. Suzuki, Control of the photocatalytic activity of TiO_2 nanoparticles by silica coating with polydiethoxysiloxane, Dye. Pigment. 76 (2008) 754-759.

[29] I.A. Siddiquey, T. Furusawa, M. Sato, N.M. Bahadur, M.N. Uddin, N. Suzuki, A rapid method for the preparation of silica-coated ZrO_2 nanoparticles by microwave irradiation, Ceram. Int. 37 (2011) 1755-1760.

[30] M.J. Uddin, M. Alam, A. Islam, S.R. Snigda, S. Das, M.M. Rahman, M.N. Uddin, C.A. Morris, R.D. Gonzalez, U. Diebold, Tailoring the photocatalytic reaction rate of a nanostructured TiO 2 matrix using additional gas phase oxygen, Int. Nano Lett. 3 (2013) 1–10.

[31] V. Calisto, M.R.M. Domingues, V.I. Esteves, Photodegradation of psychiatric pharmaceuticals in aquatic environments - Kinetics and photodegradation products, Water Res. 45 (2011) 6097-6106.

[32] A.K. Cuentas-Gallegos, R. Martínez-Rosales, M.E. Rincón, G.A. Hirata, G. Orozco, Design of hybrid materials based on carbon nanotubes and polyoxometalates, Opt. Mater. (Amst). 29 (2006) 126-133.

[33] H. Wang, H.-L. Wang, W.-F. Jiang, Solar photocatalytic degradation of 2,6-dinitro-p-cresol (DNPC) using multi-walled carbon nanotubes (MWCNTs)–TiO_2 composite photocatalysts, Chemosphere. 75 (2009) 1105-1111.

[34] G.N. Dar, A. Umar, S.A. Zaidi, A.A. Ibrahim, M. Abaker, S. Baskoutas, M.S. Al-assiri, Sensors and Actuators B : Chemical Ce-doped ZnO nanorods for the detection of hazardous chemical, Sensors Actuators B. Chem. 173 (2012) 72-78.

[35] T. Marimuthu, N. Anandhan, G. Ravi, S. Rajendran, Structural , Functional and Optical Studies on Ce Doped ZnO Nanoparticles, J. Nanosci. Nanotechnol. 2 (2014) 62-65.

[36] R.C. Deus, C.R. Foschini, F. Moura, F.G. Garcia, A.Z. Simo, Photoluminescence emission at room temperature in zinc oxide, Mater. Res. Bull. 50 (2014) 12-17.

[37] T. Zhai, S. Xie, Y. Zhao, X. Sun, X. Lu, M. Yu, M. Xu, F. Xiao, and Y. Tong, Controllable synthesis of hierarchical ZnO nanodisks for highly photocatalytic activity, CrystEngComm. 14 (2012) 1850-1855.

[38] S.R. Zhu Peining, A. Sreekumaran Nair, Yang Shengyuan, TiO_2-MWCNT rice grain-shaped nanocomposites-synthesis, characterization and photocatalysis, Mater. Res. Bull. 46 (2011) 588-595.

[39] Y. Guo, H. Wang, C. He, L. Qiu, X. Cao, Uniform Carbon-Coated ZnO Nanorods : Microwave-Assisted Preparation , Cytotoxicity , and Photocatalytic Activity, Langmuir.

25 (2009) 4678-4684.

[40] S.M.Y. A.M. El-Sayed, F.M. Ismail, M.H. Khder, M.E.M. Hassouna, Effect of CeO_2 Doping on the Structure, Electrical conductivity and ethanol gas sensing properties of nanocrystalline ZnO sensors, Int. J. Smart Sens. Intell. Syst. 5 (2012) 606-623.

[41] V.P. N. Vigeshwaran, S. Kumar, A.A. Kathe, P.V. Varadarajan, Functional finishing of cotton fabrics using zinc oxide-soluble starch nanocomposites, Nanotechnology. 17 (2006) 5087-5095.

[42] M.A. Subhan, T. Ahmed, N. Uddin, A. Kalam, K. Begum, Synthesis , characterization , PL properties , photocatalytic and antibacterial activities of nano multi-metal oxide $NiO.CeO_2.ZnO$, Spectrochim. Acta Part A Mol. Biomol. Spectrosc. 136 (2015) 824-831.

[43] M.A. Subhan, T. Ahmed, R. Awal, A.M.M. Fahim, Synthesis , structure and excitation wavelength dependent PL properties of novel nanocomposite $La_2O_2CO_3.CuO.ZnO$, Spectrochim. Acta part A Mol. Biomol. Spectrosc. 132 (2014) 550-554.

[44] M.A. Subhan, T. Ahmed, N. Uddin, Synthesis , structure , PL and photocatalytic activities of $La_2O_2CO_3.CeO_2$. ZnO fabricated by co-precipitation method, Spectrochim. Acta Part A Mol. Biomol. Spectrosc. 138 (2015) 827-833.

[45] F. Sun, X. Qiao, F. Tan, One-step microwave synthesis of Ag/ZnO nanocomposites with enhanced photocatalytic performance, J. Mater. Sci. 47 (2012) 7262-7268.

[46] T.A. Saleh, V.K. Gupta, Functionalization of tungsten oxide into MWCNT and its application for sunlight-induced degradation of rhodamine B, J. Colloid Interface Sci. 362 (2011) 337-344.

[47] J.E. Riggs, Z. Guo, D.L. Carroll, Y.P. Sun, Strong luminescence of solubilized carbon nanotubes, J. Am. Chem. Soc. 122 (2000) 5879-5880.

[48] T. Lv, L. Pan, X. Liu, T. Lu, G. Zhu, Z. Sun, Enhanced photocatalytic degradation of methylene blue by ZnO-reduced graphene oxide composite synthesized via microwave-assisted reaction, J. Alloys Compd. 509 (2011) 10086-10091.

[49] S.-Z.K.& J.M. Ya Yan, Ting Chang, Pingchun Wei, Photocatalytic Activity of Nanocomposites of ZnO and Multi-Walled Carbon Nanotubes for Dye Degradation, J. Dispers. Sci. Technol. 30 (2009) 198-203.

[50] W. Liu, M. Wang, C. Xu, S. Chen, Facile synthesis of g-C_3N_4/ZnO composite with enhanced visible light photooxidation and photoreduction properties, Chem. Eng. J. 209 (2012) 386-393.

[51] S.B. Khan, M. Faisal, M.M. Rahman, A. Jamal, Exploration of CeO_2 nanoparticles as a chemi-sensor and photo-catalyst for environmental applications, Sci. Total Environ. 409 (2011) 2987-2992.

[52] S. Kumar, A.K. Ojha, Ni, Co and Ni–Co codoping induced modification in shape, optical band gap and enhanced photocatalytic activity of CeO_2 nanostructures for photodegradation of methylene blue dye under visible light irradiation, RSC Adv. 6 (2016) 8651-8660.

[53] M. Faisal, S.B. Khan, M.M. Rahman, A. Jamal, K. Akhtar, M.M. Abdullah, Role of ZnO-CeO_2 Nanostructures as a Photo-catalyst and Chemi-sensor, J. Mater. Sci. Technol. 27 (2011) 594-600.

Fig.1. XRD patterns of the pure ZnO, Ce-doped ZnO and Ce-doped ZnO/CNT nanocomposite.

Fig.2. FESEM images of (a) pure ZnO (b) Ce-doped ZnO (c) Ce-doped ZnO/CNT nanocomposite (d) EDS spectrum of Ce-doped ZnO/CNT nanocomposite.

Fig.3. FTIR spectra of (a) Pure MWCNTs and (b) Functionalized MWCNTs.

Fig.4. FTIR spectra of (a) Pure ZnO (b) Ce-doped ZnO and (c) Ce-doped ZnO/CNT nano composite.

Fig.5. UV-vis absorption spectra of pure ZnO, Ce-doped ZnO and Ce-doped ZnO/CNT nanocomposite.

Fig.6. PL spectra of pure ZnO, Ce-doped ZnO and Ce-doped ZnO/CNT at excitation wavelength 325 nm.

Fig.7. (a) UV-Visible spectra for degradation of MB with Ce-doped ZnO/CNT photocatalyst (b) Photodegradation efficiency of pure ZnO, Ce-doped ZnO and Ce-doped ZnO/CNT photocatalysts under UV at room temperature.

Fig.8. Schematic diagram of the mechanism of photodegradation over Ce-doped ZnO/CNT nanocomposite under UV light irradiation.

.

Fig.9. Photo-catalytic degradation kinetic models: (A) Zero-order model (B) first-order model, (C) parabolic diffusion model and (D) modified Freundlich model.

Table 1 Elemental analysis of pure ZnO, Ce-doped ZnO and Ce-doped ZnO/CNT nanocomposite.

Samples	O K		Zn K		Ce K		C (CNT)	
	Weight %	Atomic %	Weight %	Atomic %	Weight %	Atomic %	Weight %	Atomic %
Pure ZnO	36.31	69.95	63.68	30.04				

Ce-doped ZnO	18.10	42.14	78.91	56.96	2.98	0.88		
Ce-doped ZnO/CNT	18.69	41.52	66.90	37.44	8.06	2.25	6.35	18.77

Table 2: Comparison of Photo-catalytic efficiency of different photocatalysts for dye degradation.

Photocatalyst	Typical parameters	Photo-catalytic activity	Reference photocatalyst ; Photo-catalytic activity	References
W-doped ZnO	Degradation of MB under UV light irradiation	[a]DE of 80%	Pure ZnO, DE of 40%	[11]
ZnO-rGO	Degradation of MB under UV light irradiation	DE of 88%	Pure ZnO; DE of 68%	[48]
ZnO-CNT	Degradation of MO under UV light irradiation	DE of 98%	Pure ZnO, DE of 35%	[49]
g-C_3N_4/ZnO	Degradation of RhB under visible light irradiation	DE of 97.4%	Pure ZnO; DE of 48%	[50]
CeO_2	Degradation of amido black under UV light irradiation	DE 45.6%		[51]
Ni-Co co doped CeO_2	Degradation of MB under visible light irradiation	DE of 60%	Pure CeO_2; DE of 20%	[52]
ZnO-CeO_2	Degradation of MB under UV light irradiation	DE of 49.65%		[53]
Ce-doped ZnO/CNT	Degradation of MB under UV light	DE of 96.37%	Pure ZnO, DE of 34.6%	**This work**

irradiation

Table 3 R^2 photo-catalytic kinetic models applied to pure ZnO, Ce-doped ZnO and Ce-doped ZnO/CNT nanocomposite.

Photoctalytic degradation Kinetics models	**Pure ZnO**		**Ce-doped ZnO**		**Ce-doped ZnO/CNT**	
	R^2	k	R^2	k	R^2	k
Zero-order model	0.2991	0.00259	0.3928	0.00312	0.3531	0.00333
First-order model	0.9123	0.00072	0.9852	0.00211	0.9916	0.00579
Parabolic diffusion model	0.9806	0.1936	0.9847	0.2209	0.9796	0.1865
Modified Freundlich model	0.8508	0.043	0.959	0.089	0.9822	0.079

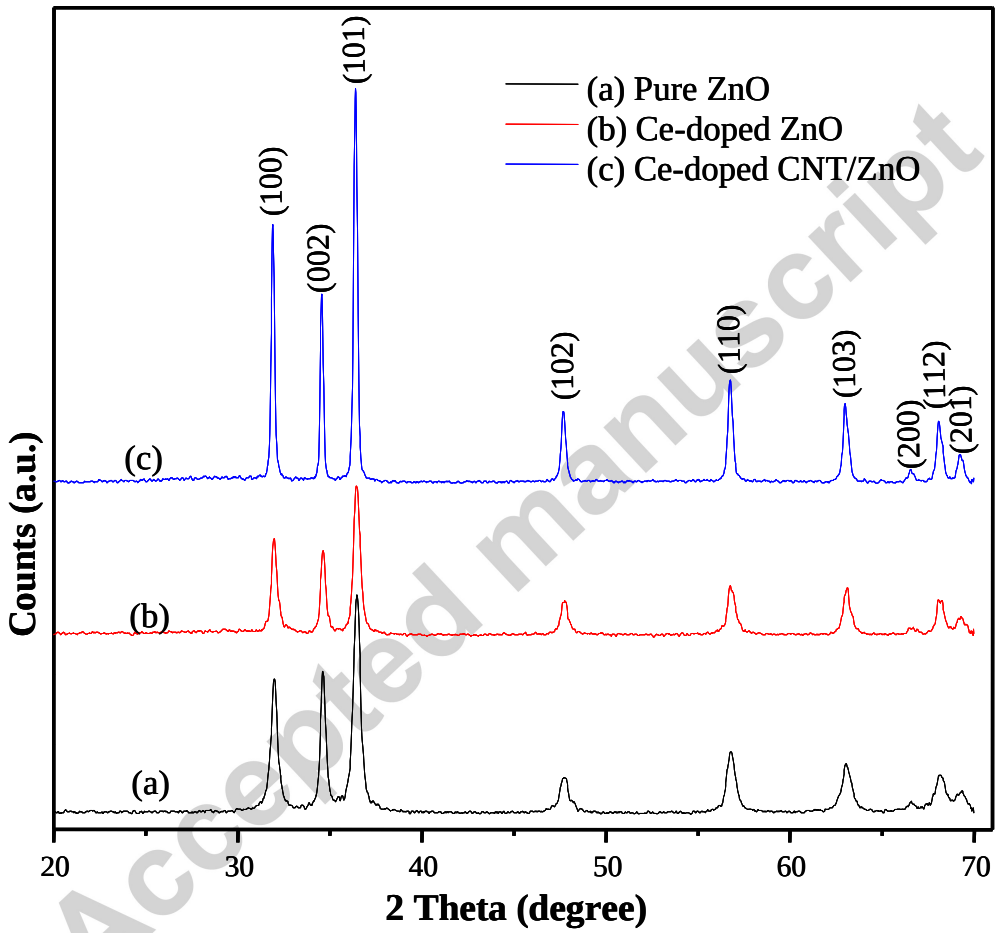

Fig. 1

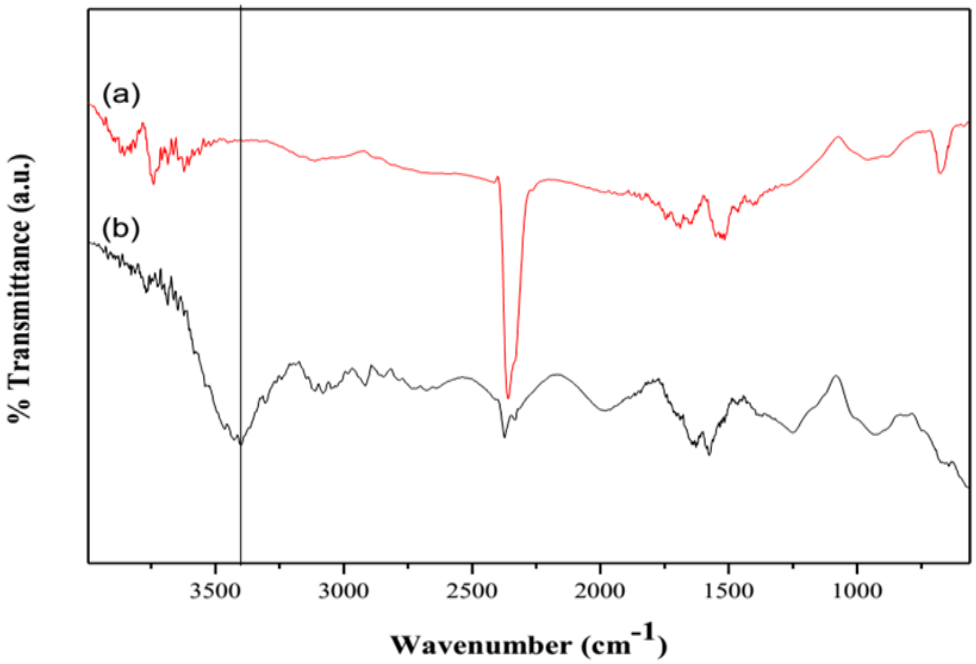

Fig. 2

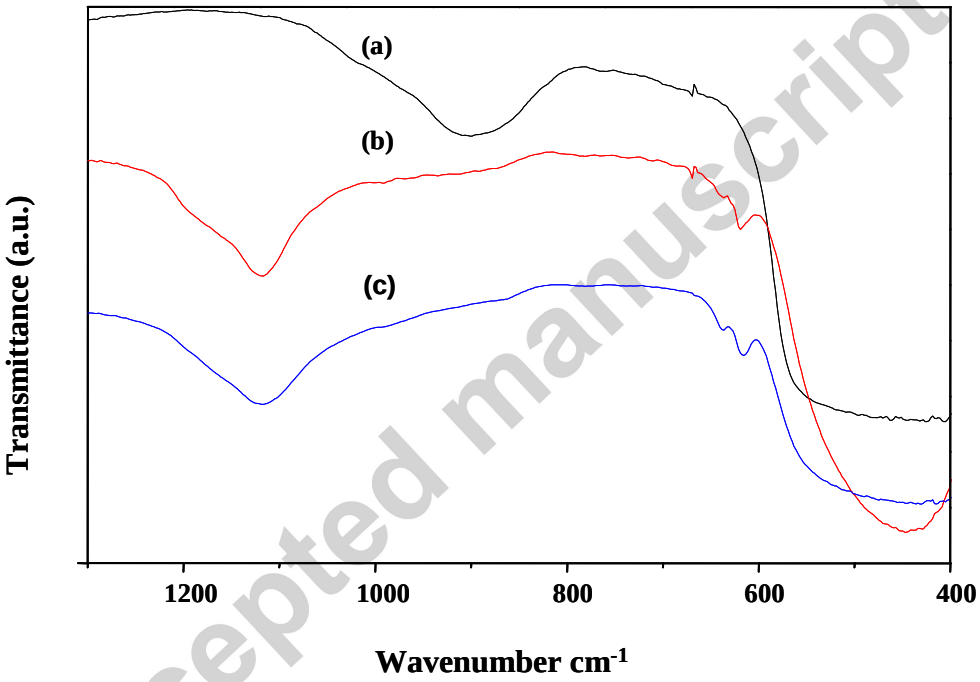

Fig. 3

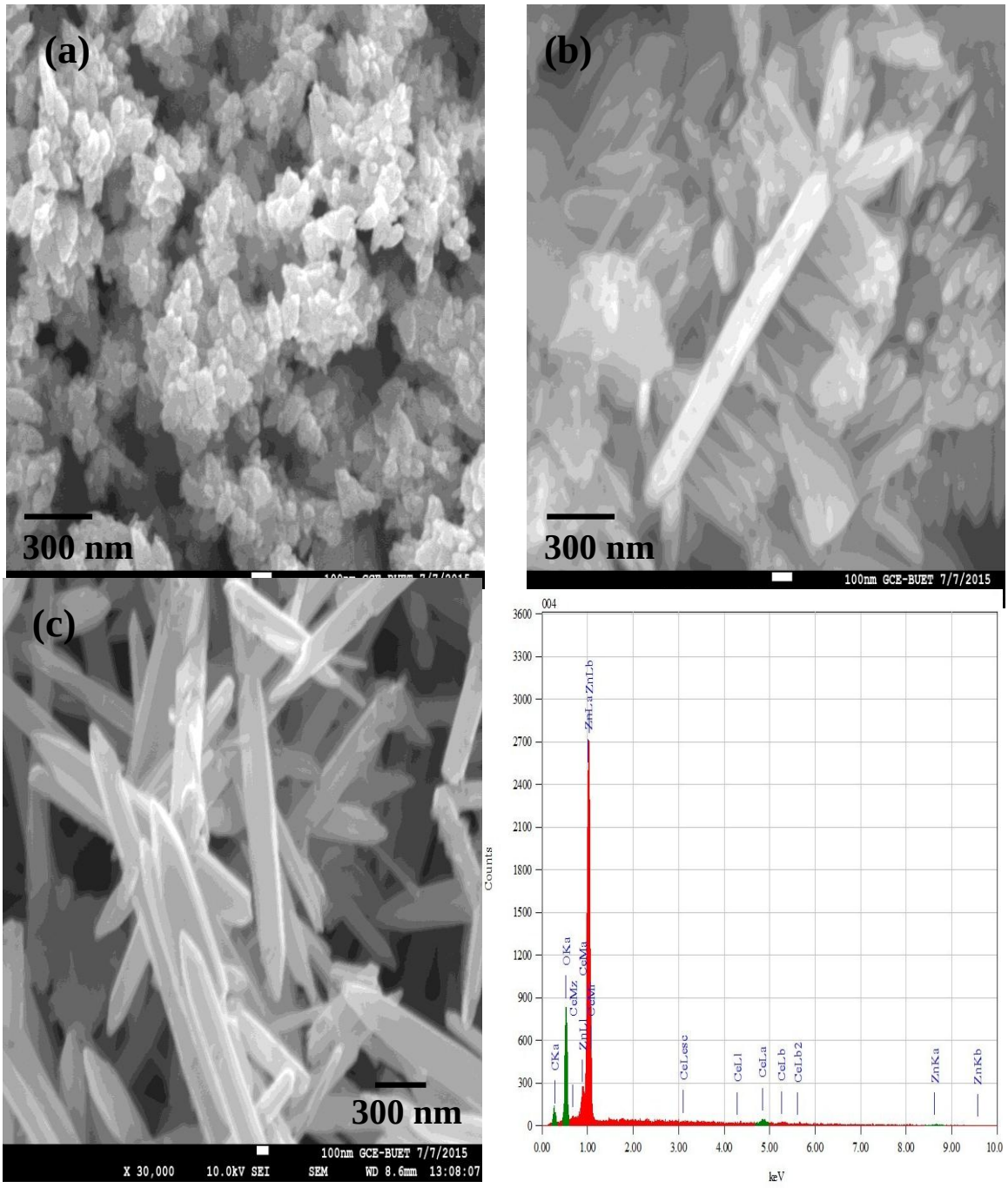

Fig. 4

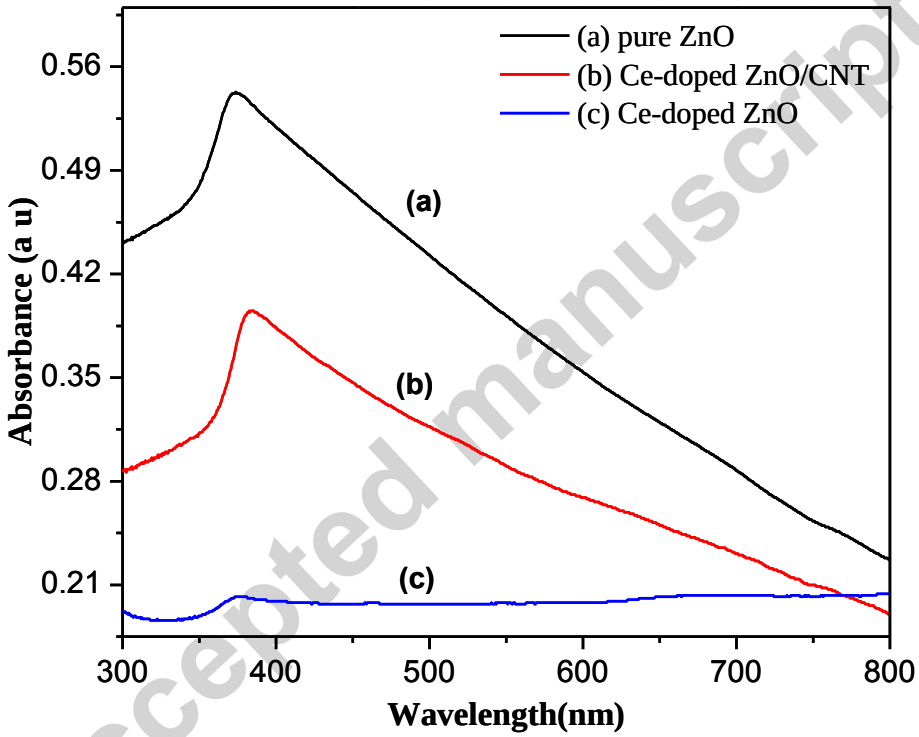

Fig. 5

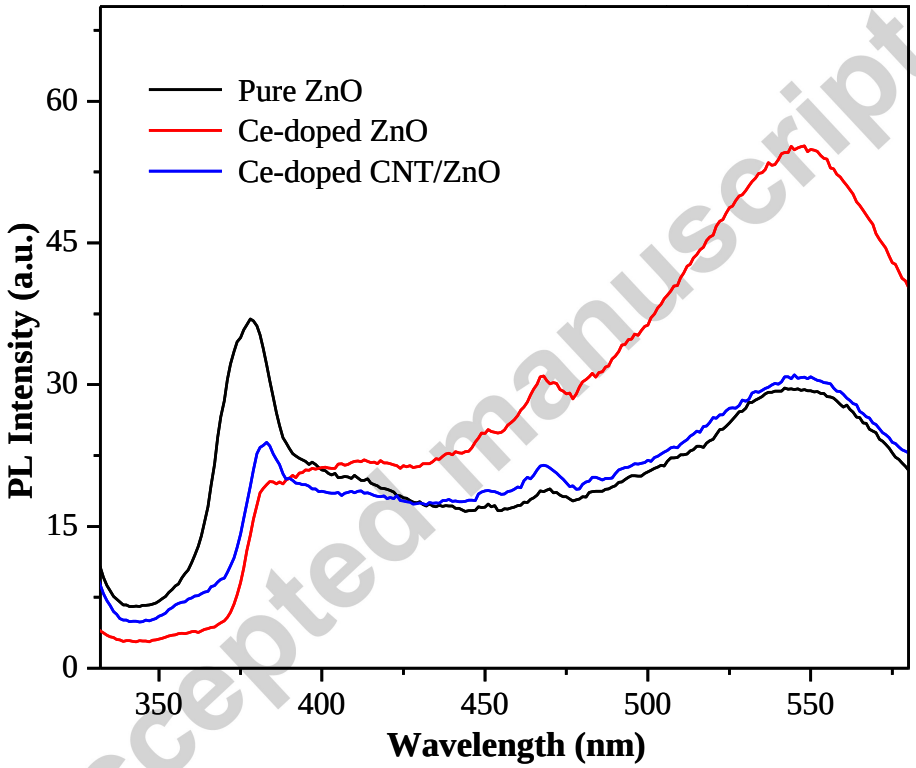

Fig. 6

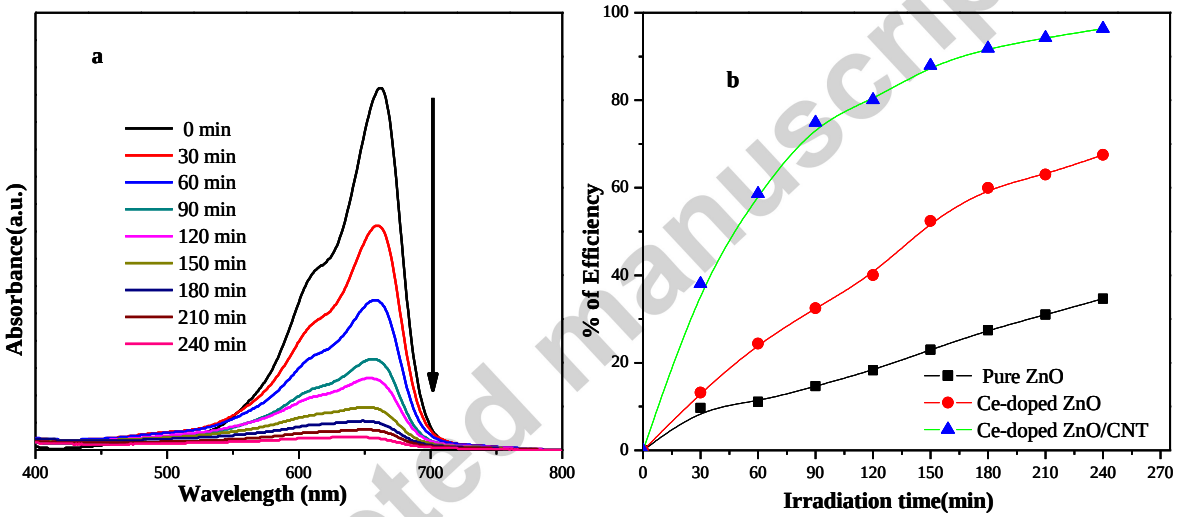

Fig. 7

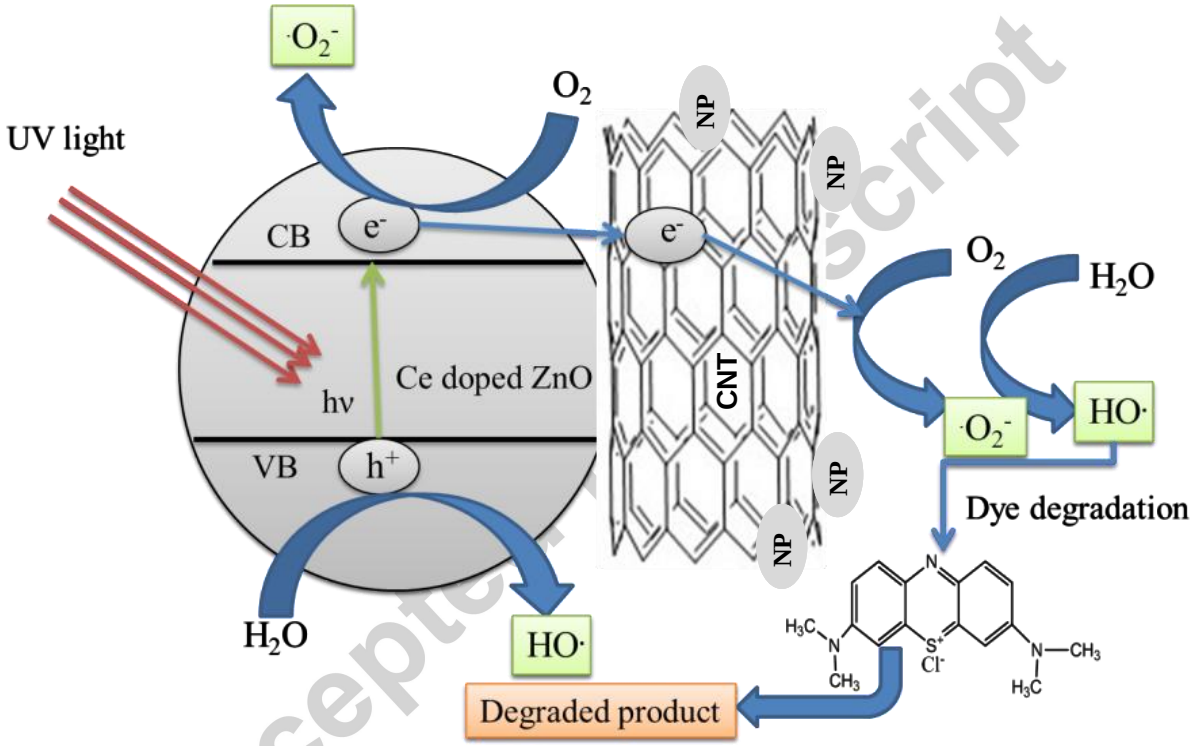

Fig. 8

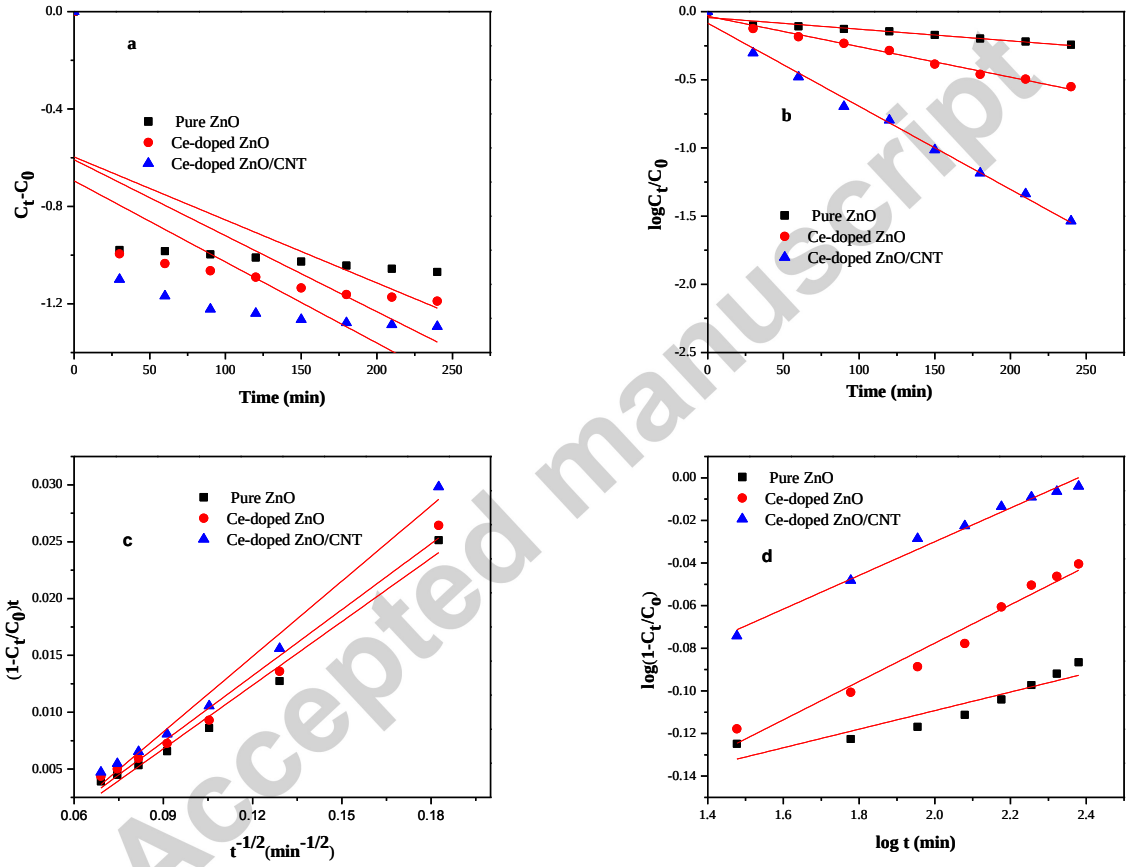

Fig. 9